

Title page

**Optogenetic inhibition of spinal inhibitory neurons facilitates mechanical responses
of spinal wide dynamic range neurons and causes mechanical hypersensitivity**

**Yuka Fujiwara^{a,b}, Keisuke Koga^{a,*}, Nozomu H. Nakamura^c, Keishi Maruo^b, Toshiya
Tachibana^{b,*}, Hidemasa Furue^a**

^a Department of Neurophysiology, Hyogo Medical University, 1-1 Mukogawa,
Nishinomiya 663-8501, Japan

^b Department of Orthopaedic Surgery, Hyogo Medical University, 1-1 Mukogawa,
Nishinomiya 663-8501, Japan

^c Department of Physiology, Hyogo Medical University, 1-1, Mukogawa, Nishinomiya
663-8501, Japan

^{*}Corresponding authors

Keisuke Koga, Ph.D.

Department of Neurophysiology, Hyogo Medical University, Nishinomiya 663-8501,
Japan.

19 Tel: +81-798-45-6988, FAX: +81-798-45-6989, e-mail: ke-koga@hyo-med.ac.jp

20

21 Toshiya Tachibana, Ph D.

22 Department of Orthopaedic Surgery, Hyogo Medical University, Nishinomiya 663-8501,

23 Japan

24 Tel: +81-798-45-6452, Fax: +81-798-45-6453, e-mail: tachi@hyo-med.ac.jp

25

26

27 **Highlights**

28 • Optogenetic inhibition of spinal inhibitory neurons induced mechanical
29 hypersensitivity

30 • Opto-disinhibition enhanced sensory responses of wide dynamic range (WDR) neurons

31 • Mirogabalin inhibited abnormal firing of WDR neurons and contributed to analgesia

32

33 **Abstract**

34 Inhibitory interneurons in the spinal dorsal horn (DH) play a major role in regulating
35 innocuous and noxious information. Reduction in inhibitory synaptic transmission is
36 thought to contribute to the development of touch-evoked pain (allodynia), a common
37 symptom of neuropathic pain. However, it is not fully understood how inhibitory neurons
38 in the DH regulate sensory responses in surrounding neurons and modulate sensory
39 transmission. In this study, we established a novel experimental method to analyze
40 temporal activity of DH neurons during the optogenetically induced disinhibition state by
41 combining extracellular recording and optogenetics. We investigated how specific and
42 temporally restricted dysfunction of DH inhibitory neurons affected spinal neuronal
43 activities evoked by cutaneous mechanical stimulation. In behavioral experiments, the
44 specific and temporally restricted spinal optogenetic suppression of DH inhibitory
45 neurons induced mechanical hypersensitivity. Furthermore, this manipulation enhanced
46 the mechanical responses of wide dynamic range (WDR) neurons, which are important
47 for pain transmission, in response to brush and von Frey stimulation but not in response
48 to nociceptive pinch stimulation. In addition, we examined whether a neuropathic pain
49 medication, mirogabalin, suppressed these optogenetically induced abnormal pain
50 responses. We found that mirogabalin treatment attenuated the abnormal firing responses

51 of WDR neurons and mechanical hypersensitivity. These results suggest that temporally
52 restricted and specific reduction of spinal inhibitory neuronal activity facilitates the
53 mechanical responses of WDR neurons, resulting in neuropathic-like mechanical
54 allodynia which can be suppressed by mibogabalin. Our optogenetic methods could be
55 useful for developing novel therapeutics for neuropathic pain.

1 **Keywords**

2 Pain; optogenetics; inhibitory interneurons; mechanical hypersensitivity; somatosensory
3 system; wide dynamic range neuron

4

5 **Abbreviations**

6 WDR, Wide dynamic range; DH, Dorsal horn; GABA, Gamma-aminobutyric acid; Vgat,
7 Vesicular GABA transporter; AAV, Adeno-associated virus; EYFP, Enhanced yellow
8 fluorescent protein; PBS, Phosphate buffered saline; PFA, Paraformaldehyde; aCSF,
9 Artificial cerebrospinal fluid; PWT, Paw withdrawal threshold; RVM, Rostral
10 ventromedial medulla; NMDAR, N-methyl-D-aspartate receptor

1. Introduction

Somatosensory information transmitted from the periphery is processed in the spinal dorsal horn (DH) and transmitted to the brain via spinal projection neurons (Braz et al., 2014; Todd, 2010). DH interneurons are crucial for the modulation and transmission of sensory information and are classified into two main types: excitatory and inhibitory. Balance between excitation and inhibition is critical for maintaining normal sensory functions. Loss of inhibitory signaling in the DH is a major contributor to neuropathic pain and the development of touch-evoked pain (allodynia) (Coull et al., 2003; Inoue and Tsuda, 2018; Moore et al., 2002b). Recent studies have identified spinal inhibitory neuronal subtypes important for sensory modulation. Ablation and/or inhibition of these spinal neuronal subtypes induce hypersensitivity to specific sensory inputs and facilitates excitatory neuronal activity and synaptic transmission (Boyle et al., 2023; Duan et al., 2014; Foster et al., 2015; Petitjean et al., 2015; Tashima et al., 2021). However, the effects of dysfunction of DH inhibitory neurons on spinal neuronal activity and mechanical sensory responses remain unclear.

DH neurons are classified according to their responses to sensory stimuli. Wide dynamic range (WDR) neurons preferentially respond to noxious mechanical stimuli at higher firing rates rather than to innocuous mechanical stimuli (Dado et al., 1994; Price

and Browe, 1973). WDR neurons are located in both the superficial and deep dorsal horns and are considered crucial for encoding nociceptive intensity and nociceptive transmission. Facilitation of WDR neuronal activity and plastic changes in those excitatory synapses are involved in pain hypersensitivity under chronic pain conditions (Suzuki and Dickenson, 2006; Tan et al., 2012). However, whether the mechanical responses of WDR neurons are modulated by inhibitory interneurons, and the corresponding mechanisms remain undetermined.

Employing optogenetics, a technique enabling manipulation of neuronal signaling processes with precise timing and local control, we investigated the effects of specific inhibition of inhibitory interneurons on the mechanical sensitivity and sensory responses of WDR neurons. We also examined whether a neuropathic pain medication could suppress these abnormal pain responses.

2. Material and Methods

2.1. Animals

Male and female *Vgat-Cre* mice (B6J-Slc32a1tm2(cre)lowl/MwarJ, Stock No: 028862, The Jackson Laboratory) (Vong et al., 2011) were used for the experiments. All mice were 8–12 weeks old at the start of each experiment, housed at $22 \pm 1^\circ\text{C}$ with a 12 h light/dark cycle with food, and provided ad libitum access to food and water. All animal studies were reviewed and approved by the Animal Care and Use Committee of Hyogo Medical University. All animal experiments were performed in accordance with the institutional guidelines and complied the ethical guidelines of the International Association for the Study of Pain.

2.2. Microinjection

We used the previously reported method (Koga et al., 2023; Kohro et al., 2015). Briefly, under anesthesia, the skin was incised in the midline at Th11-L4 and the vertebral column was clamped. The paraspinal muscles around the right side of the interspaces of Th13-L1 were removed, and the dura mater and arachnoid membrane were carefully incised to create a small window. rAAV solutions (AAV9-EF1 α -FLEX-eNpHR3.0-EYFP (Addgene, 26966-AAV9) (Gradinaru et al., 2010) or AAV9-EF1 α -FLEX-mCherry (Kohro et al., 2020) (kindly gifted by Prof. Makoto Tsuda) were injected into the DH (200–300 μm in

depth from the surface). We used mice 3–4 weeks or more after the injection of AAV vectors.

2.3. Immunohistochemistry

Immunohistochemical experiments were performed according to the methods described previously (Koga et al., 2023; Kohro et al., 2020). Mice were deeply anesthetized by intraperitoneal (i.p.) injection of urethane (1.2–1.5 mg/kg) and perfused transcardially with phosphate buffered saline (PBS), followed by ice-cold 4% paraformaldehyde (PFA) in PBS. The L3–L4 segments of spinal cord were removed, postfixed in the same fixative overnight at 4°C, and subsequently left immersed in 30% sucrose solution for 2–3 nights at 4°C. Transverse spinal cord sections (40 µm thick) were prepared using a cryostat (CM3050S, Leica) and stained with the following antibodies: a polyclonal goat anti-PAX2 (1:500; AF3364; R&D Systems) as the primary antibody and Donkey anti-goat CyTM₃ (1:500, AB_2307351, Jackson ImmunoResearch) as the secondary antibody. Single optical sections were obtained using a water-immersion objective lens (LD LCI Plan Apo 25x/0.8 W, Zwiss) or a 63x water-immersion objective lens (C-Apo 63x/1.2 W, Zwiss) and a confocal laser microscope (LSM780, Carl Zeiss).

2.4. Slice patch-clamp recording

We used the methods described in our previous studies (Koga et al., 2017; Yasaka et al.,

2007). Mice were deeply anesthetized with i.p. injection of 1.2–1.5 mg/kg urethane (0.24 mg/ml). The lumbosacral spinal cord was removed and placed to cold, preoxygenated, high-sucrose artificial cerebrospinal fluid containing 250 mM sucrose, 2.5 mM KCl, 2 mM CaCl_2 , 2 mM MgCl_2 , 1.2 mM NaH_2PO_4 , 25 mM NaHCO_3 , and 11 mM glucose. A single parasagittal spinal cord slice (250–300 μm thick) was prepared using a vibrating microtome (NLS-MT; Dosaka) from each mice that had received the spinal injection, and the slice were maintained in an artificial cerebrospinal fluid solution (aCSF) containing 125 mM NaCl, 2.5 mM KCl, 2 mM CaCl_2 , 1 mM MgCl_2 , 1.25 mM NaH_2PO_4 , 26 mM NaHCO_3 , and 20 mM glucose at room temperature (23–26 °C) for at least 30 min. The spinal cord slice was then placed into a recording chamber that was continuously superfused with aCSF solution at a flow rate of 4–6 mL/min at 27–30 °C. The patch pipettes were filled with an internal solution containing: 135 mM K-gluconate, 0.5 mM CaCl_2 , 2 mM MgCl_2 , 5 mM KCl, 5 mM EGTA, 5 mM Mg-ATP, and HEPES (pH 7.2 adjusted with KOH). Whole-cell patch-clamp recordings were made from lamina II eNpHR-EYFP-positive neurons. The MultiClamp 700A amplifier and pCLAMP 10.4 acquisition software (Molecular Devices) were used for recording. The data were digitized using an analog-to-digital converter (Digidata 1321A; Molecular Devices), stored by a data acquisition software (Clampex version 8.2; Molecular Devices), and

analyzed using a software package (Clampfit version10.4; Molecular Devices). Light induced currents were recorded under voltage-clamp conditions at a holding potential of -50 mV. Discharge patterns were examined under current-clamp conditions by passing hyperpolarizing and depolarizing current pulses through the recording electrode from the resting membrane potential.

2.5. Extracellular recording

Analysis of *in vivo* electrophysiology was performed as described in our previous reports (Funai et al., 2014; Furue et al., 1999; Kawai et al., 2021). The mice were deeply anesthetized with intraperitoneal 1.2–1.5 g/kg urethane (0.24 mg/ml). The skin of the back was incised up to T13–L2, the perispinal tissues and muscles were removed, and a Th13–L2 laminectomy was performed. The mice were fixed using a custom-made stereotaxic apparatus (Narishige). The surface of the exposed spinal cord was continuously perfused with Krebs' solution containing: 117 mM NaCl, 3.6 mM KCl, 2.5 mM CaCl₂, 1.2 mM MgCl₂, 1.2 mM NaH₂PO₄, 25 mM NaHCO₃, and 11 mM glucose equilibrated with 95% O₂ and 5% CO₂ at 38 ± 0.5°C at a flow rate of 5–10 ml/min at 38 ± 0.5 °C. The dura mater and the pia-arachnoid membrane were removed using a 30G needle. A tungsten electrode (10 MΩ impedance, #210977, FHC) was placed into the DH (100–300 μm from the exposed spinal cord surface) and multi-unit activity was

extracellularly recorded using an AC differential amplifier (EX1, Dagan). The signal was subjected to bandpass-filtering at 300–3 kHz and sampled at 20 kHz. The recorded signals were spike-sorted using Offline Sorter software (version3, Plexon) (Funai et al., 2014). Light stimulation (0.24–10 mW, for 10 s) was applied to the spinal cord surface. Brush, von Frey and pinch stimulations were applied to the right hindpaws before and during light stimulation. We characterized WDR neurons as those whose response to pinch stimulation was 1 to 3-fold higher than their response to brush stimulation. Mirogabalin was perfused with 60 μ M on the surface of the spinal cord. Only cells, whose responses were enhanced by light stimulation, were used for the mirogabalin treatment study.

2.6. Fiber-optic implantation

Fiber-optic implantation was performed according to the method described previously (Christensen et al., 2016). The mice were deeply anesthetized with a cocktail of anesthetic drugs (0.3 mg/kg medetomidine hydrochloride, 4 mg/kg midazolam, and 5 mg/kg butorphanol). The skin was incised up to Th11–L3, and tissue and muscles around the spinal column were removed. The vertebrae were clamped and a hole was drilled through the vertebral body at the right center of T1. A ϕ 200 μ m core cannula (with a tip length of \sim 0.5 mm, prepared using a ceramic ferrule [CFX230-10, Thorlabs]) was placed and fixed to the drilled vertebrae using adhesive and dental cement. The incised skin was

subsequently sutured.

2.7. Behavioral analysis

To assess mechanical hypersensitivity, mice were placed individually in an opaque acrylic box ($6 \times 6 \times 6$ cm) on a wire mesh and habituated for ~1 h to allow acclimatization to the experimental environment. Light stimulation was applied to the spinal cord via optic fiber for 10 s. Calibrated von Frey filaments (0.02-2.0 g North Coast Medical) were applied to the plantar surfaces of the hindpaws of mice from below the mesh floor with or without light stimulation, and the 50 % paw withdrawal threshold (PWT) was determined using the up-down method (Chaplan et al., 1994; Kohro et al., 2020). Mirogabalin was administered intraperitoneally at dose of 3 mg/kg and 10 mg/kg.

2.8. Statistical analysis

Mice were randomly assigned to each experimental group. For various analyses, we repeated the experiment in multiple cohorts of animals. The experimenters were not blinded. In the figure legends, we provide details on the sample numbers, statistical tests used, and the results of all statistical analyses for each experiment and all statistical comparisons. Statistical analyses were performed using the Prism 9 software (GraphPad). All data are presented as the mean \pm standard error of the mean (SEM). The statistical significance of the differences was determined using one-way repeated measures ANOVA

149 with Dunnett's test and two-way repeated measures ANOVA with Sidak's test and
150 Bonferroni's multiple comparisons test. Differences were considered statistically
151 significant at $p < 0.05$.

3. Results

3.1. Specific transduction of eNpHR3.0 into the DH inhibitory neuron.

To control spinal inhibitory neuronal activity in a temporally restricted and specific manner, we used *Vgat-Cre* mice, expressing Cre recombinase downstream of the endogenous vesicular GABA transporter-encoding gene (*Vgat*) (Vong et al., 2011) and an adeno-associated virus (AAV) vector that enabled halorhodopsin (eNpHR3.0) expression in a Cre-dependent manner (Gradinaru et al., 2010). The AAV vector was microinjected into the spinal cord of *Vgat-cre* mice to express halorhodopsin specifically in inhibitory neurons (Fig. 1A). Mice expressing mCherry in the same manner were used as the controls. In fluorescent immunostaining experiment, enhanced yellow fluorescent protein (EYFP) fused with halorhodopsin was expressed in the superficial area of the DH, and a part of the EYFP signals were merged with PAX2, an inhibitory neuron marker in the DH (Ross et al., 2010), but not all the EYFP signals were colocalized with PAX2 (Fig. 1B, *upper*). It is considered by the difference of cellular localization of eNpHR and PAX2, i.e., eNpHR is a light-activated Cl⁻ pump located in cellular surface (Gradinaru et al., 2008), while Pax2 is located in nuclei. To investigate the precise localization of these proteins, we performed imaging experiments with high magnification scans, and the Pax2-positive nuclei were surrounded by EYFP signals, suggesting eNpHR-EYFP was

expressed in cell surface of Pax2-positive inhibitory neurons (Fig. 1B, *lower*). Next, we examined the firing pattern of EYFP-positive cells by slice patch clamp recording, and all the recorded cells exhibited tonic firing responses to current injection (6/6, Fig. 1C, *left*), which is characteristic of inhibitory neurons (Todd, 2010; Yasaka et al., 2010), suggesting that halorhodopsin was selectively expressed in inhibitory neurons. Light stimulation (667 μ m wavelength) under the voltage-clamp mode induced a large outward current, which increased in correlation with the light intensity (Fig. 1C, *middle* and *right*). These results confirmed that halorhodopsin was specifically and functionally expressed in inhibitory neurons.

3.2. Behavioral analysis of the effects of light-induced disinhibition on PWT of the Vgat-eNpHR mice.

To investigate the behavioral effect of optical inhibition of inhibitory interneurons, we performed the von Frey test using Vgat-eNpHR and Vgat-mCherry mice with an optical fiber attached to the L1 vertebra (Fig. 2A) (Uhelski et al., 2017). Light stimulation (at 5 and 10 mW) significantly decreased PWT ipsilateral to the virus vector injection side in the Vgat-eNpHR mice, but did not affect PWT of the contralateral side (Fig. 2B, *left*). In contrast, no significant differences were observed in Vgat-mCherry control group (Fig.

2B, *right*). These results suggest that temporally restricted inhibition of inhibitory interneurons is sufficient to induce mechanical hypersensitivity.

3.3 *In vivo* extracellular recording analysis of the effects of light stimulation on mechanical sensory responses of WDR neurons.

To examine the effect of light stimulation on spinal neuronal activity and sensory responses, we performed *in vivo* extracellular recordings from WDR neurons in the DH (100–300 μ m from the exposed DH surface) of Vgat-eNpHR mice (Fig. 3A). We applied brush (Fig. 3B), von Frey (10 g; Fig. 3C), and pinch (Fig. 3D) stimulations to the right hindpaw without or with light stimulation (0.3–10 mW) to the halorhodopsin-expressing spinal cord of Vgat-eNpHR mice. Firing responses to brush and von Frey (10 g) stimulations were significantly enhanced in WDR neurons by light stimulation in correlation with light intensity, while responses to pinch stimulation and basal firing rate were not altered by light stimulation (Fig. 3E). On the other hand, these alterations were not observed in Vgat-mCherry mice (Fig. 3F). These results indicate that temporally restricted disinhibition by light stimulation induces abnormal firing responses in WDR neurons.

3.4 Effects of mirogabalin administration on the enhanced mechanical responses of WDR neurons induced by the light-induced disinhibition.

Since disinhibition is a crucial mechanism of neuropathic pain, we investigated the effects of mirogabalin, an $\alpha_2\delta$ -1 ligand used for the treatment of neuropathic pain (Kato et al., 2021; Kitano et al., 2019). We performed *in vivo* extracellular recordings from WDR neurons and examined the effects of mirogabalin administration to the spinal cord on the light-induced sensory facilitation. Consistent with previous data, responses to brush (Fig. 4A, B) and von Frey (10 g) (Fig. 4C, D) were significantly enhanced upon light stimulation. The enhancement of sensory responses by light stimulation was suppressed by mirogabalin administration, whereas the basal responses without light stimulation were not affected by mirogabalin. In contrast, the responses to pinch stimulation were not significantly altered by light stimulation or mirogabalin administration (Fig. 4E, F). These results suggest that the sensory responses facilitated by light stimulation were alleviated by mirogabalin administration.

3.5 Behavioral analysis of the effect of mirogabalin administration on the mechanical hypersensitivity induced by light stimulation.

To examine the effect of mirogabalin on withdrawal behavior, we intraperitoneally

224 administered 3 or 10 mg/kg of mirogabalin or saline (control) to Vgat-eNpHR mice, and
225 performed the von Frey test for 1 to 5 h after the administration. The decrease in PWT on
226 the side of the virus vector injection induced by light stimulation was significantly
227 ameliorated by treatment with 3 or 10 mg/kg of mirogabalin compared to that observed
228 in control saline-treated mice. (Fig. 5, *left*). No significant differences were observed in
229 the contralateral paw between the two groups (Fig. 5, *right*), suggesting that mirogabalin
230 did not affect basal mechanical sensitivity. According to these results, mirogabalin
231 administration alleviated the mechanical hypersensitivity induced by disinhibition.

4. Discussion

DH inhibitory interneurons are important for the transmission and regulation of pain information, and loss of inhibitory transmission is considered one of the crucial mechanisms underlying the development of neuropathic pain (Sivilotti and Woolf, 1994; Todd, 2010). Specifically, the administration of inhibitory neurotransmitter antagonists into the DH induces severe mechanical hypersensitivity and spontaneous nociceptive behaviors, and the specific silencing and/or ablation of subsets of inhibitory interneurons induces abnormal sensory responses and synaptic transmission (Duan et al., 2014; Foster et al., 2015; Koga et al., 2017; Tsukamoto et al., 2010). However, whether temporally restricted inhibition is sufficient to induce pain hypersensitivity, and the underlying neuronal mechanisms remain unknown. Using optogenetic methods that enables us to control neuronal activity with cellular and millisecond-temporal precision (Boyden et al., 2005), we found that temporally restricted and specific suppression of inhibitory neurons in the DH induced mechanical hypersensitivity and enhanced the mechanical responses of WDR neurons. Further studies are needed to investigate the effect of the inhibition of specific populations of inhibitory or excitatory neurons on spinal sensory responses and transmission.

250 Alteration in DH neuronal activity have been reported in the neuropathic pain model
251 (Suzuki and Dickenson, 2006; Zain and Bonin, 2019). However, whether the activity of
252 the same population of DH neurons is affected by neuropathic pain conditions remains
253 unknown. To overcome this limitation, we established the method to analyze alteration of
254 DH neuronal activity during the disinhibition state using halorhodopsin to specifically
255 inhibit inhibitory neurons in the DH by light stimulation, imitating a neuropathic pain
256 state. Using this method, we continuously recorded the activity of the same neurons in
257 mice with and without temporally restricted disinhibition. According to our results, the
258 specific and temporally restricted spinal optogenetic suppression of inhibitory neurons
259 enhanced mechanical responses in WDR neurons in the DH (100–300 μ m from the DH
260 surface including superficial and deep laminae). These data was consistent with previous
261 studies suggested that the excitatory synaptic transmission in lamina II neurons and NK1-
262 positive neurons in superficial and deep laminae was enhanced by disinhibition (Baba et
263 al., 2003; Torsney and MacDermott, 2006). Although inhibitory neurotransmitter
264 antagonists facilitate mechanical response of DH neurons toward brush, touch, and pinch
265 stimulations (Keller et al., 2007), these manipulations inhibit inhibitory transmission from
266 not only the synaptic activity of spinal inhibitory interneurons, but also descending
267 inhibitory neurotransmission from the rostral ventromedial medulla (Francois et al., 2017;

268 Kato et al., 2006), and tonic GABA signaling (Ataka and Gu, 2006). In contrast to the
269 previous report, our optogenetic suppression performed in this study facilitated selective
270 WDR neuronal responses to brush and von Frey stimulations, but not to pinch stimulation.
271 Further studies were needed to elucidate the mechanism for controlling pinch response in
272 DH neurons. However, since we selectively inhibited the activity of spinal inhibitory
273 interneurons, the results suggest that inhibitory interneurons actively participate in the
274 regulation of the mechanical responses of WDR neurons.

275

276 Neuropathic pain, which is caused by a lesion or disease of the somatosensory nervous
277 system, reduces patients' activities of daily living, and is often refractory to current
278 treatments (Bannister et al., 2020). Gabapentinoids such as, pregabalin, gabapentin, and
279 mirogabalin, are commonly used to treat neuropathic pain. Gabapentinoids bind to $\alpha_2\delta-1$,
280 a subunit of voltage-gated calcium channels, and alleviate altered spinal calcium-
281 mediated neurotransmitter release and pain hypersensitivity in neuropathic pain condition
282 (Dooley et al., 2007; Taylor, 2009). A previous study have reported that administration of
283 pregabalin significantly alleviated the hypersensitivity of dorsal horn WDR neurons and
284 mechanical allodynia in rats with spared nerve injury (Ding et al., 2014). We found that
285 mirogabalin administration did not affect spinal neurotransmission without light-induced

286 disinhibition, but the enhanced mechanical responses in the light-evoked disinhibition
287 state were suppressed by mibogabalin administration, suggesting that $\alpha_2\delta$ -1 recruited in
288 disinhibition state could be involved in these enhanced activities. We previously reported
289 that $\alpha_2\delta$ -1 in the spinal cord is important for pain facilitation and the enhanced release of
290 excitatory neurotransmitter in neuropathic pain and disinhibition states (Koga et al., 2023).
291 Furthermore, application of a gabapentinoid inhibits synaptically evoked NMDAR-
292 mediated excitatory synaptic transmission in the presence of inhibitory neurotransmitter
293 antagonists (Moore et al., 2002a). These reports support our assumption and suggest that
294 $\alpha_2\delta$ -1 in DH neurons is important to facilitate the mechanical responses induced by
295 optogenetic disinhibition. However, further investigations are needed to confirm our
296 hypothesis and to identify the detailed mechanisms of action of gabapentinoids.

297 **5. Conclusions**

298 We established a novel experimental method that enabled us to analyze the temporal
299 activity of DH neurons during optogenetically induced disinhibition. Using this method,
300 we demonstrated the specific optogenetic suppression of inhibitory interneuron activity
301 induced mechanical hypersensitivity and abnormal neuronal sensory responses in WDR
302 neurons. Furthermore, our results suggested that $\alpha_2\delta$ -1 ligand, a therapeutic reagent for
303 neuropathic pain, exerted analgesic effects by suppressing the abnormal firings of WDR
304 neurons.

Funding

This work was conducted in collaboration with Daiichi Sankyo Co., Ltd. This work was supported by the following grants. JSPS KAKENHI Grants (JP20H04043 (H.F.), JP23K18441 (H.F.), JP20K16133 (K.K.), JP22K15206 (K.K.)), the Hyogo Innovative Challenge grant (H.F.), the Hyogo College of Medicine Grant for Research Promotion 2021 and 2023 (K.K.), and “Hyogo Medical University Diversity Grant for Research Promotion” under MEXT Funds for the Development of Human Resources in Science and Technology, Initiative for Realizing Diversity in the Research Environment (H.F.).

CRedit author statement

Y.F.: validation, formal analysis, investigation, data curation, writing – original draft, visualization. K.K.: conceptualization, methodology, investigation, writing – original draft, project administration, funding acquisition. N.N.: resources, writing – review & editing. K.M.: writing – review & editing, supervision. T.T.: writing – review & editing, supervision. H.F.: conceptualization, writing – review & editing, supervision, funding acquisition. All the authors have read and approved the final version of the manuscript.

Declaration of competing interest

H.F. received research funding from Daiichi Sankyo Co., Ltd. The funder was not involved in the study design, collection, analysis, interpretation of data, the writing of this article or the decision to submit it for publication. All authors declare no other competing interests.

Data availability

The original data supporting the conclusions of this article will be made available by the corresponding authors upon reasonable request.

Acknowledgements

We thank the joint-use research facilities and the Center for Comparative Medicine of Hyogo Medical University for use of facilities. We thank Prof. Makoto Tsuda for providing the AAV9-EF1a-FLEX-mCherry vector.

336 **References**

337 Ataka, T., Gu, J. G., 2006. Relationship between tonic inhibitory currents and phasic
338 inhibitory activity in the spinal cord lamina II region of adult mice. *Mol Pain* 2, 36,
339 10.1186/1744-8069-2-36.

340 Baba, H., Ji, R. R., Kohno, T., Moore, K. A., Ataka, T., Wakai, A., Okamoto, M., Woolf,
341 C. J., 2003. Removal of GABAergic inhibition facilitates polysynaptic A fiber-mediated
342 excitatory transmission to the superficial spinal dorsal horn. *Mol Cell Neurosci* 24, 818-
343 830, 10.1016/s1044-7431(03)00236-7.

344 Bannister, K., Sachau, J., Baron, R., Dickenson, A. H., 2020. Neuropathic Pain:
345 Mechanism-Based Therapeutics. *Annu Rev Pharmacol Toxicol* 60, 257-274,
346 10.1146/annurev-pharmtox-010818-021524.

347 Boyden, E. S., Zhang, F., Bamberg, E., Nagel, G., Deisseroth, K., 2005. Millisecond-
348 timescale, genetically targeted optical control of neural activity. *Nat Neurosci* 8, 1263-
349 1268, 10.1038/nn1525.

350 Boyle, K. A., Polgar, E., Gutierrez-Mecinas, M., Dickie, A. C., Cooper, A. H., Bell, A.
351 M., Jumolea, E., Casas-Benito, A., Watanabe, M., Hughes, D. I., Weir, G. A., Riddell, J.
352 S., Todd, A. J., 2023. Neuropeptide Y-expressing dorsal horn inhibitory interneurons gate

353 spinal pain and itch signalling. *Elife* 12, 86633, 10.7554/eLife.86633.

354 Braz, J., Solorzano, C., Wang, X., Basbaum, A. I., 2014. Transmitting pain and itch
355 messages: a contemporary view of the spinal cord circuits that generate gate control.
356 *Neuron* 82, 522-536, 10.1016/j.neuron.2014.01.018.

357 Chaplan, S. R., Bach, F. W., Pogrel, J. W., Chung, J. M., Yaksh, T. L., 1994. Quantitative
358 assessment of tactile allodynia in the rat paw. *J Neurosci Methods* 53, 55-63,
359 10.1016/0165-0270(94)90144-9.

360 Christensen, A. J., Iyer, S. M., François, A., Vyas, S., Ramakrishnan, C., Vesuna, S.,
361 Deisseroth, K., Scherrer, G., Delp, S. L., 2016. In Vivo Interrogation of Spinal
362 Mechanosensory Circuits. *Cell Rep* 17, 1699-1710, 10.1016/j.celrep.2016.10.010.

363 Coull, J. A., Boudreau, D., Bachand, K., Prescott, S. A., Nault, F., Sik, A., De Koninck,
364 P., De Koninck, Y., 2003. Trans-synaptic shift in anion gradient in spinal lamina I neurons
365 as a mechanism of neuropathic pain. *Nature* 424, 938-942, 10.1038/nature01868.

366 Dado, R. J., Katter, J. T., Giesler, G. J., Jr., 1994. Spinothalamic and spinohypothalamic
367 tract neurons in the cervical enlargement of rats. II. Responses to innocuous and noxious
368 mechanical and thermal stimuli. *J Neurophysiol* 71, 981-1002, 10.1152/jn.1994.71.3.981.

369 Ding, L., Cai, J., Guo, X. Y., Meng, X. L., Xing, G. G., 2014. The antiallodynic action of
370 pregabalin may depend on the suppression of spinal neuronal hyperexcitability in rats
371 with spared nerve injury. *Pain Res Manag* 19, 205-211, 10.1155/2014/623830.

372 Dooley, D. J., Taylor, C. P., Donevan, S., Feltner, D., 2007. Ca²⁺ channel α 2delta
373 ligands: novel modulators of neurotransmission. *Trends Pharmacol Sci* 28, 75-82,
374 10.1016/j.tips.2006.12.006.

375 Duan, B., Cheng, L., Bourane, S., Britz, O., Padilla, C., Garcia-Campmany, L., Krashes,
376 M., Knowlton, W., Velasquez, T., Ren, X., Ross, S., Lowell, B. B., Wang, Y., Goulding,
377 M., Ma, Q., 2014. Identification of spinal circuits transmitting and gating mechanical pain.
378 *Cell* 159, 1417-1432, 10.1016/j.cell.2014.11.003.

379 Foster, E., Wildner, H., Tudeau, L., Haueter, S., Ralvenius, W. T., Jegen, M., Johannssen,
380 H., Hosli, L., Haenraets, K., Ghanem, A., Conzelmann, K. K., Bosl, M., Zeilhofer, H. U.,
381 2015. Targeted ablation, silencing, and activation establish glycinergic dorsal horn
382 neurons as key components of a spinal gate for pain and itch. *Neuron* 85, 1289-1304,
383 10.1016/j.neuron.2015.02.028.

384 Francois, A., Low, S. A., Sypek, E. I., Christensen, A. J., Sotoudeh, C., Beier, K. T.,
385 Ramakrishnan, C., Ritola, K. D., Sharif-Naeini, R., Deisseroth, K., Delp, S. L., Malenka,

386 R. C., Luo, L., Hantman, A. W., Scherrer, G., 2017. A Brainstem-Spinal Cord Inhibitory
387 Circuit for Mechanical Pain Modulation by GABA and Enkephalins. *Neuron* 93, 822-839
388 e826, 10.1016/j.neuron.2017.01.008.

389 Funai, Y., Pickering, A. E., Uta, D., Nishikawa, K., Mori, T., Asada, A., Imoto, K., Furue,
390 H., 2014. Systemic dexmedetomidine augments inhibitory synaptic transmission in the
391 superficial dorsal horn through activation of descending noradrenergic control: an in vivo
392 patch-clamp analysis of analgesic mechanisms. *Pain* 155, 617-628,
393 10.1016/j.pain.2013.12.018.

394 Furue, H., Narikawa, K., Kumamoto, E., Yoshimura, M., 1999. Responsiveness of rat
395 substantia gelatinosa neurones to mechanical but not thermal stimuli revealed by in vivo
396 patch-clamp recording. *J Physiol* 521 Pt 2, 529-535, 10.1111/j.1469-7793.1999.00529.x.

397 Gradinaru, V., Thompson, K. R., Deisseroth, K., 2008. eNpHR: a *Natronomonas*
398 halorhodopsin enhanced for optogenetic applications. *Brain Cell Biol* 36, 129-139,
399 10.1007/s11068-008-9027-6.

400 Gradinaru, V., Zhang, F., Ramakrishnan, C., Mattis, J., Prakash, R., Diester, I., Goshen,
401 I., Thompson, K. R., Deisseroth, K., 2010. Molecular and cellular approaches for
402 diversifying and extending optogenetics. *Cell* 141, 154-165, 10.1016/j.cell.2010.02.037.

403 Inoue, K., Tsuda, M., 2018. Microglia in neuropathic pain: cellular and molecular
404 mechanisms and therapeutic potential. *Nat Rev Neurosci* 19, 138-152,
405 10.1038/nrn.2018.2.

406 Kato, G., Yasaka, T., Katafuchi, T., Furue, H., Mizuno, M., Iwamoto, Y., Yoshimura, M.,
407 2006. Direct GABAergic and glycinergic inhibition of the substantia gelatinosa from the
408 rostral ventromedial medulla revealed by in vivo patch-clamp analysis in rats. *J Neurosci*
409 26, 1787-1794, 10.1523/JNEUROSCI.4856-05.2006.

410 Kato, J., Inoue, T., Yokoyama, M., Kuroha, M., 2021. A review of a new voltage-gated
411 Ca^{2+} channel $\alpha(2)\delta$ ligand, mirogabalin, for the treatment of peripheral
412 neuropathic pain. *Expert Opin Pharmacother* 22, 2311-2322,
413 10.1080/14656566.2021.1958780.

414 Kawai, M., Imaizumi, K., Ishikawa, M., Shibata, S., Shinozaki, M., Shibata, T.,
415 Hashimoto, S., Kitagawa, T., Ago, K., Kajikawa, K., Shibata, R., Kamata, Y., Ushiba, J.,
416 Koga, K., Furue, H., Matsumoto, M., Nakamura, M., Nagoshi, N., Okano, H., 2021.
417 Long-term selective stimulation of transplanted neural stem/progenitor cells for spinal
418 cord injury improves locomotor function. *Cell Rep* 37, 110019,
419 10.1016/j.celrep.2021.110019.

420 Keller, A. F., Beggs, S., Salter, M. W., De Koninck, Y., 2007. Transformation of the output
421 of spinal lamina I neurons after nerve injury and microglia stimulation underlying
422 neuropathic pain. *Mol Pain* 3, 27, 10.1186/1744-8069-3-27.

423 Kitano, Y., Wakimoto, S., Tamura, S., Kubota, K., Domon, Y., Arakawa, N., Saito, M.,
424 Sava, B., Buisson, B., 2019. Effects of mirogabalin, a novel ligand for the alpha(2)delta
425 subunit of voltage-gated calcium channels, on N-type calcium channel currents of rat
426 dorsal root ganglion culture neurons. *Pharmazie* 74, 147-149, 10.1691/ph.2019.8833.

427 Koga, K., Kanehisa, K., Kohro, Y., Shiratori-Hayashi, M., Tozaki-Saitoh, H., Inoue, K.,
428 Furue, H., Tsuda, M., 2017. Chemogenetic silencing of GABAergic dorsal horn
429 interneurons induces morphine-resistant spontaneous nocifensive behaviours. *Sci Rep* 7,
430 4739, 10.1038/s41598-017-04972-3.

431 Koga, K., Kobayashi, K., Tsuda, M., Kubota, K., Kitano, Y., Furue, H., 2023. Voltage-
432 gated calcium channel subunit alpha(2)delta-1 in spinal dorsal horn neurons contributes
433 to aberrant excitatory synaptic transmission and mechanical hypersensitivity after
434 peripheral nerve injury. *Front Mol Neurosci* 16, 1099925, 10.3389/fnmol.2023.1099925.

435 Kohro, Y., Matsuda, T., Yoshihara, K., Kohno, K., Koga, K., Katsuragi, R., Oka, T.,
436 Tashima, R., Muneta, S., Yamane, T., Okada, S., Momokino, K., Furusho, A., Hamase,

437 K., Oti, T., Sakamoto, H., Hayashida, K., Kobayashi, R., Horii, T., Hatada, I., Tozaki-
438 Saitoh, H., Mikoshiba, K., Taylor, V., Inoue, K., Tsuda, M., 2020. Spinal astrocytes in
439 superficial laminae gate brainstem descending control of mechanosensory
440 hypersensitivity. *Nat Neurosci* 23, 1376-1387, 10.1038/s41593-020-00713-4.

441 Kohro, Y., Sakaguchi, E., Tashima, R., Tozaki-Saitoh, H., Okano, H., Inoue, K., Tsuda,
442 M., 2015. A new minimally-invasive method for microinjection into the mouse spinal
443 dorsal horn. *Sci Rep* 5, 14306, 10.1038/srep14306.

444 Moore, K. A., Baba, H., Woolf, C. J., 2002a. Gabapentin-- actions on adult superficial
445 dorsal horn neurons. *Neuropharmacology* 43, 1077-1081, 10.1016/s0028-
446 3908(02)00226-5.

447 Moore, K. A., Kohno, T., Karchewski, L. A., Scholz, J., Baba, H., Woolf, C. J., 2002b.
448 Partial peripheral nerve injury promotes a selective loss of GABAergic inhibition in the
449 superficial dorsal horn of the spinal cord. *J Neurosci* 22, 6724-6731, 20026611.

450 Petitjean, H., Pawlowski, S. A., Fraine, S. L., Sharif, B., Hamad, D., Fatima, T., Berg, J.,
451 Brown, C. M., Jan, L. Y., Ribeiro-da-Silva, A., Braz, J. M., Basbaum, A. I., Sharif-Naeini,
452 R., 2015. Dorsal Horn Parvalbumin Neurons Are Gate-Keepers of Touch-Evoked Pain
453 after Nerve Injury. *Cell Rep* 13, 1246-1257, 10.1016/j.celrep.2015.09.080.

454 Price, D. D., Browe, A. C., 1973. Responses of spinal cord neurons to graded noxious and
455 non-noxious stimuli. *Brain Res* 64, 425-429, 10.1016/0006-8993(73)90199-6.

456 Ross, S. E., Mardinly, A. R., McCord, A. E., Zurawski, J., Cohen, S., Jung, C., Hu, L.,
457 Mok, S. I., Shah, A., Savner, E. M., Tolias, C., Corfas, R., Chen, S., Inquimbert, P., Xu,
458 Y., McInnes, R. R., Rice, F. L., Corfas, G., Ma, Q., Woolf, C. J., Greenberg, M. E., 2010.
459 Loss of inhibitory interneurons in the dorsal spinal cord and elevated itch in *Bhlhb5*
460 mutant mice. *Neuron* 65, 886-898, 10.1016/j.neuron.2010.02.025.

461 Sivilotti, L., Woolf, C. J., 1994. The contribution of GABAA and glycine receptors to
462 central sensitization: disinhibition and touch-evoked allodynia in the spinal cord. *J*
463 *Neurophysiol* 72, 169-179, 10.1152/jn.1994.72.1.169.

464 Suzuki, R., Dickenson, A. H., 2006. Differential pharmacological modulation of the
465 spontaneous stimulus-independent activity in the rat spinal cord following peripheral
466 nerve injury. *Exp Neurol* 198, 72-80, 10.1016/j.expneurol.2005.10.032.

467 Tan, A. M., Samad, O. A., Fischer, T. Z., Zhao, P., Persson, A. K., Waxman, S. G., 2012.
468 Maladaptive dendritic spine remodeling contributes to diabetic neuropathic pain. *J*
469 *Neurosci* 32, 6795-6807, 10.1523/JNEUROSCI.1017-12.2012.

470 Tashima, R., Koga, K., Yoshikawa, Y., Sekine, M., Watanabe, M., Tozaki-Saitoh, H.,
471 Furue, H., Yasaka, T., Tsuda, M., 2021. A subset of spinal dorsal horn interneurons crucial
472 for gating touch-evoked pain-like behavior. *Proc Natl Acad Sci U S A* 118, 2021220118,
473 10.1073/pnas.2021220118.

474 Taylor, C. P., 2009. Mechanisms of analgesia by gabapentin and pregabalin--calcium
475 channel $\alpha 2$ -delta [Cavalpha2-delta] ligands. *Pain* 142, 13-16,
476 10.1016/j.pain.2008.11.019.

477 Todd, A. J., 2010. Neuronal circuitry for pain processing in the dorsal horn. *Nat Rev*
478 *Neurosci* 11, 823-836, 10.1038/nrn2947.

479 Torsney, C., MacDermott, A. B., 2006. Disinhibition opens the gate to pathological pain
480 signaling in superficial neurokinin 1 receptor-expressing neurons in rat spinal cord. *J*
481 *Neurosci* 26, 1833-1843, 10.1523/JNEUROSCI.4584-05.2006.

482 Tsukamoto, M., Kiso, T., Shimoshige, Y., Aoki, T., Matsuoka, N., 2010. Spinal
483 mechanism of standard analgesics: evaluation using mouse models of allodynia. *Eur J*
484 *Pharmacol* 634, 40-45, 10.1016/j.ejphar.2010.02.025.

485 Uhelski, M. L., Bruce, D. J., Séguéla, P., Wilcox, G. L., Simone, D. A., 2017. In vivo

486 optogenetic activation of Na. J Neurophysiol 117, 2218-2223, 10.1152/jn.00083.2017.

487 Vong, L., Ye, C., Yang, Z., Choi, B., Chua, S., Jr., Lowell, B. B., 2011. Leptin action on
488 GABAergic neurons prevents obesity and reduces inhibitory tone to POMC neurons.
489 Neuron 71, 142-154, 10.1016/j.neuron.2011.05.028.

490 Yasaka, T., Kato, G., Furue, H., Rashid, M. H., Sonohata, M., Tamae, A., Murata, Y.,
491 Masuko, S., Yoshimura, M., 2007. Cell-type-specific excitatory and inhibitory circuits
492 involving primary afferents in the substantia gelatinosa of the rat spinal dorsal horn in
493 vitro. J Physiol 581, 603-618, 10.1113/jphysiol.2006.123919.

494 Yasaka, T., Tiong, S. Y. X., Hughes, D. I., Riddell, J. S., Todd, A. J., 2010. Populations of
495 inhibitory and excitatory interneurons in lamina II of the adult rat spinal dorsal horn
496 revealed by a combined electrophysiological and anatomical approach. Pain 151, 475-
497 488, 10.1016/j.pain.2010.08.008.

498 Zain, M., Bonin, R. P., 2019. Alterations in evoked and spontaneous activity of dorsal
499 horn wide dynamic range neurons in pathological pain: a systematic review and analysis.
500 Pain 160, 2199-2209, 10.1097/j.pain.0000000000001632.

Figure Legends

Figure 1, AAV-mediated transduction of eNpHR3.0 in spinal cord dorsal horn inhibitory neurons.

(A) Schematic illustrations of a Cre-dependent eNpHR expression vector (*left*) and mice with adeno-associated virus (AAV) microinjection (Vgat-eNpHR mice) (*right*). (B) Representative single optical sections showing eNpHR-EYFP expression (*green*) and PAX2 (*red*), obtained using a 25x objective lens (*upper*) and a 63x objective lens (*lower*). White arrows indicate the Pax2-positive cells surrounded by eNpHR-YFP signals. (C) Representative traces obtained from eNpHR-expressing neurons, showing AP discharge induced by current injection (*left*), outward currents recorded with varying intensity (0.3, 1, 3, 5, 10 mW) of light stimulation under the voltage-clamp mode (*middle*), and the results of the analysis (*right*).

Figure 2, Behavioral analysis of the effects of light stimulation on PWT of the Vgat-eNpHR mice.

(A) Mice with an optical fiber implanted onto the DH. (B) Summary showing PWT during 5 and 10 mW light stimulations in Vgat-eNpHR3.0 (*left*) and control (Vgat-mCherry) (*right*) groups. (Two-way repeated measurements ANOVA post-hoc Sidak's test,

eNpHR3.0 (n = 11 mice, Group $F_{(1, 60)} = 117.6$; **** $p < 0.0001$, treatment $F_{(2, 60)} = 24.84$; **** $p < 0.0001$, interaction $F_{(2, 60)} = 17.62$; **** $p < 0.0001$ (Pre; $p = 0.41$, 5 mW; **** $p < 0.0001$, 10 mW; **** $p < 0.0001$)), mCherry (n = 5 mice, Group $F_{(1, 24)} = 0.3802$; $p = 0.5433$, treatment $F_{(2, 24)} = 2.279$; $p = 0.1241$, interaction $F_{(2, 24)} = 0.1539$; $p = 0.8582$ (Pre; $p = 0.84$, 5 mW; $p > 0.99$, 10 mW; $p = 0.97$)). Mechanical hypersensitivity was induced in Vgat-eNpHR3.0 mice by the light stimulations.

Figure 3, Effects of light stimulation on mechanical sensory responses elicited in WDR neurons.

(A) Schematic diagrams of *in vivo* extracellular recording from the lumbar dorsal horn and light stimulation. (B-D) Representative traces showing WDR neuronal firings in response to brush, 10 g von Frey and pinch stimulation before (Pre, *left*) and under the light stimulation (3 mW, *middle*, 10 mW, *right*). In those recording, two units were isolated from each traces and indicated as 1 and 2 (*left*, temporally magnified traces), and their unit activities were shown above each trace. (E-F) Summary showing the effects of light stimulation on WDR neuronal mechanical responses in Vgat-eNpHR (E) and Vgat-mCherry (F) mice. (One-way repeated measurements ANOVA post-hoc Dunnett's test, eNpHR3.0; n = 13 (brush: $F_{(1.942, 23.31)} = 6.204$, 0.3 mW; $p = 0.10$, 3 mW; ** $p = 0.0074$, 5

537 mW; **p = 0.0090, 10 mW; *p = 0.023, von Frey 10 g: $F_{(2.427, 29.12)} = 6.450$, 0.3 mW; p =
 538 0.29, 3 mW; *p = 0.014, 5 mW; *p = 0.046, 10 mW; **p = 0.0059, pinch: $F_{(1.876, 22.51)} =$
 539 2.185, 0.3 mW; p = 0.98, 3 mW; p = 0.94, 5 mW; p = 0.34, 10 mW; p = 0.10), mCherry;
 540 n = 8 (brush: $F_{(1.926, 13.48)} = 2.889$, 0.3 mW; p = 0.077, 3 mW; p = 0.48, 5 mW; p = 0.11,
 541 10 mW; p = 0.93, von Frey 10 g: $F_{(2.650, 18.55)} = 1.118$, 0.3 mW; p = 0.80, 3 mW; p = 0.91,
 542 5 mW; p = 0.54, 10 mW; p = 0.38, pinch: $F_{(2.113, 14.79)} = 0.5904$, 0.3 mW; p = 0.58, 3 mW;
 543 p = 0.51 5 mW; p = 0.22, 10 mW; p > 0.99) *p < 0.05, **p < 0.01). Innocuous mechanical
 544 responses of WDR neurons were enhanced by light stimulation in Vgat-eNpHR3.0 mice.

545

546 **Figure 4, Effects of mirogabalin administration on enhanced sensory responses in**
 547 **WDR neurons by disinhibition.**

548 (A,C,E) Representative traces of dorsal horn neuronal firings in response to brush, 10 g
 549 von Frey and pinch stimulation before (Pre, *left*), and under the action of light stimulation
 550 (Light, *middle*) in the absence and presence (Mirogabalin+Light, *right*) of mirogabalin
 551 (60 μ M) administrated onto the spinal surface. Summary of firing frequency of WDR
 552 neuronal responses before and under the light stimulation, and effects of mirogabalin on
 553 WDR neuronal responses under the light stimulation. In those recording, two units were
 554 isolated from each trace and indicated as 1 and 2 (*left*, temporally magnified traces), and

their unit activities were shown above each trace. (B,D,F) Summary showing the effect of mirogabalin on the light-induced enhanced responses to mechanical stimulation in WDR neurons (One-way repeated measurements ANOVA post-hoc Dunnett's test, brush (n =19): $F_{(1.571, 28.27)} = 9.189$, Pre vs. Light; $**p = 0.001$, Pre vs. Mirogabalin; $p = 0.99$, Pre vs. Mirogabalin+Light; $p = 0.72$, von Frey (n = 20): $F_{(1.991, 37.84)} = 4.329$, Pre vs. Light; $*p = 0.049$, Pre vs. Mirogabalin; $p = 0.98$, Pre vs. Mirogabalin+Light; $p = 0.30$, pinch (n = 23); $F_{(1.569, 34.52)} = 2.097$, Pre vs. Light; $**p = 0.63$, Pre vs. Mirogabalin; $p = 0.24$, Pre vs. Mirogabalin+Light; $p = 0.10$, $*p < 0.05$, $**p < 0.01$). Mirogabalin treatment alleviated the enhanced mechanical responses of WDR neurons induced by light stimulation.

Figure 5, Effects of mirogabalin administration on PWT during light stimulation.

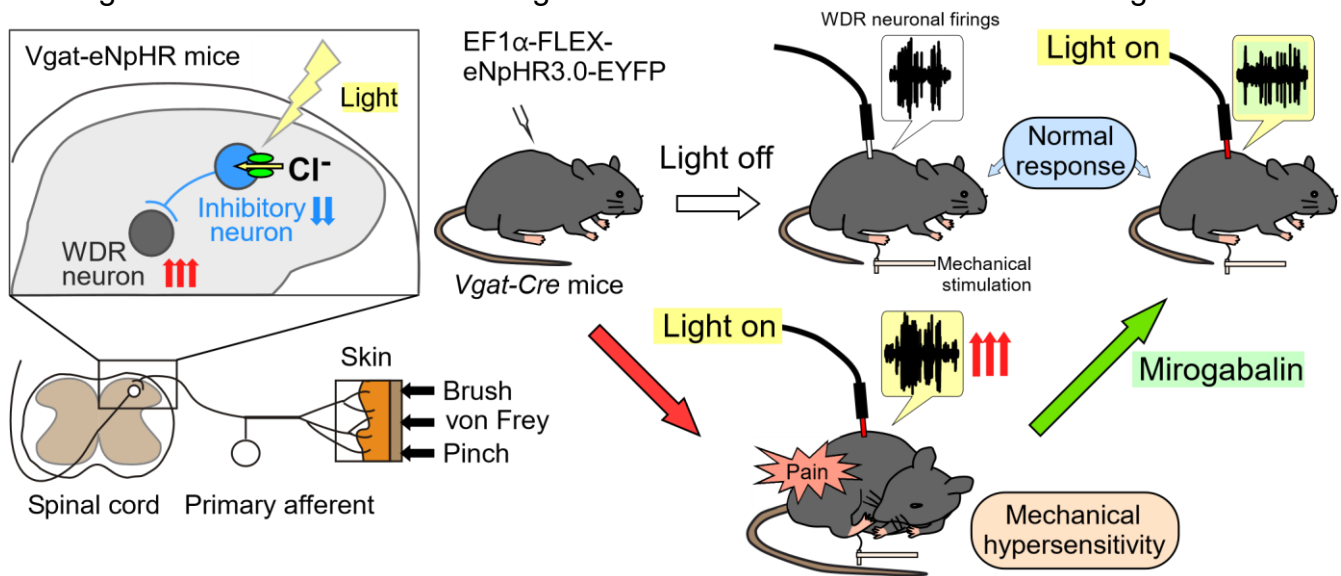
Analysis of PWT ipsilateral (*left*) and contralateral (*right*) to spinal AAV injection side in Vgat-eNpHR mice during light stimulation after intraperitoneal administration of saline (control), 3 mg/kg, or 10 mg/kg of mirogabalin. (saline; n = 9 mice, mirogabalin 3 mg/kg; n = 6, mirogabalin 10 mg/kg; n = 6, two-way ANOVA post-hoc Bonferroni's test) (Contralateral: Group $F_{(2, 125)} = 2.725$; $p = 0.0694$, treatment $F_{(6, 125)} = 0.5259$; $p = 0.7878$, interaction $F_{(12, 125)} = 0.5639$; $p = 0.8673$, Pre (saline vs. 3 mg/kg ; $p > 0.99$, saline vs. 10 mg/kg; $p > 0.99$), Pre+Light (saline vs. 3 mg/kg ; $p > 0.99$, saline vs. 10 mg/kg; $p > 0.99$),

573 1h (saline vs. 3 mg/kg; $p > 0.99$, saline vs. 10 mg/kg; $p > 0.99$), 2h (saline vs. 3 mg/kg; p
574 > 0.99 , saline vs. 10 mg/kg; $p = 0.31$), 3h (saline vs. 3 mg/kg; $p > 0.99$, saline vs. 10
575 mg/kg; $p > 0.99$), 4h (saline vs. 3 mg/kg; $p = 0.72$, saline vs. 10 mg/kg; $p = 0.16$), 5h
576 (saline vs. 3 mg/kg; $p = 0.77$, saline vs. 10 mg/kg; $p = 0.055$)) (Injection side: Group $F_{(2, 125)}$
577 $= 13.62$; $p < 0.0001$, treatment $F_{(6, 125)} = 58.07$; $p < 0.0001$, interaction $F_{(12, 125)} = 2.954$;
578 $p = 0.0012$, Pre (saline vs. 3 mg/kg; $p = 0.38$, saline vs. 10 mg/kg; $p = 0.45$), Pre+Light
579 (saline vs. 3 mg/kg; $p > 0.99$, saline vs. 10 mg/kg; $p > 0.99$), 1h (saline vs. 3 mg/kg; $p >$
580 0.99 , saline vs. 10 mg/kg; $p > 0.99$), 2h (saline vs. 3 mg/kg; $p = 0.69$, saline vs. 10 mg/kg;
581 $p = 0.087$), 3h (saline vs. 3 mg/kg; $p = 0.17$, saline vs. 10 mg/kg; $*p = 0.015$), 4h (saline
582 vs. 3 mg/kg; $***p = 0.0004$, saline vs. 10 mg/kg; $****p < 0.0001$), 5h (saline vs. 3 mg/kg;
583 $**p = 0.0045$, saline vs. 10 mg/kg; $****p < 0.0001$) $*p < 0.05$, $**p < 0.01$, $***p < 0.001$,
584 $****p < 0.0001$). Mirogabalin treatment alleviated the mechanical hypersensitivity
585 induced by light stimulation.

Graphical abstract

How does attenuation of inhibitory neuronal activity change spinal sensory responses and nociceptive behaviors?

- Optogenetic inhibition of spinal inhibitory neurons induced mechanical hypersensitivity
- Opto-disinhibition enhanced sensory responses of spinal wide dynamic range (WDR) neurons
- Mirogabalin inhibited abnormal firing of WDR neurons and contributed to analgesia



Conclusion

Temporally restricted and specific reduction of spinal inhibitory neuronal activity facilitates the mechanical responses of WDR neurons, resulting in neuropathic-like mechanical allodynia which can be suppressed by mirogabalin.

Figure1

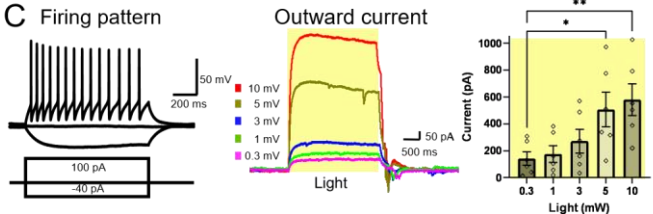
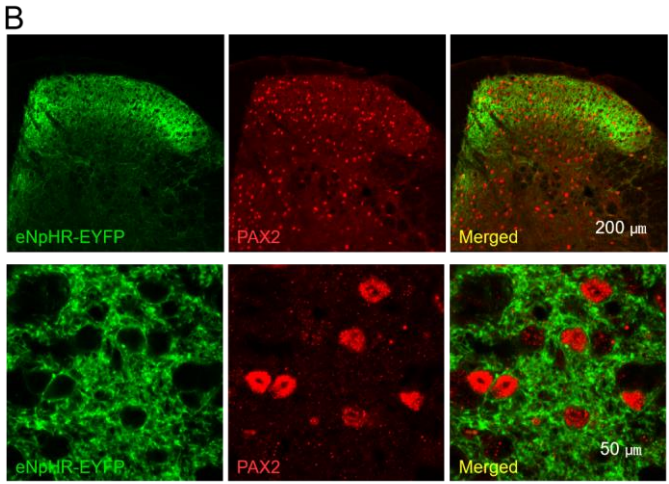
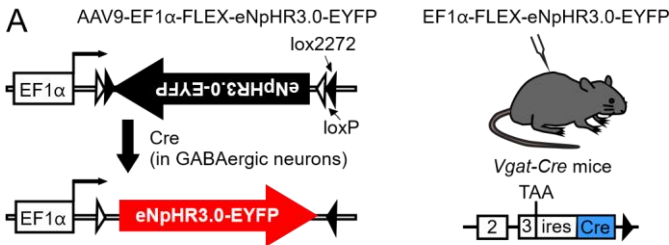


Figure2

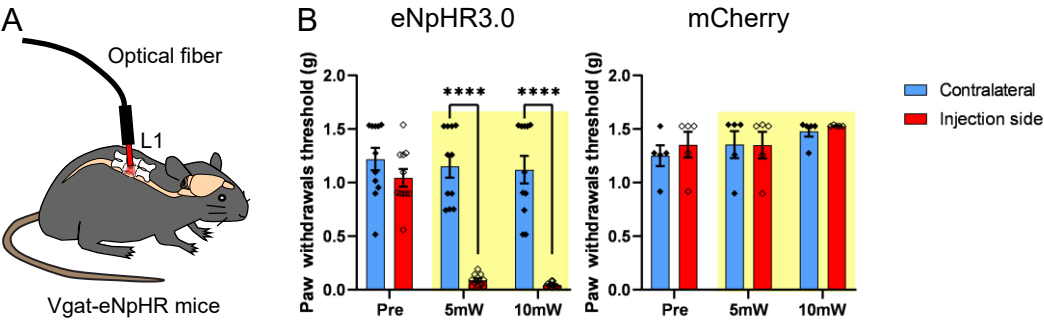


Figure3

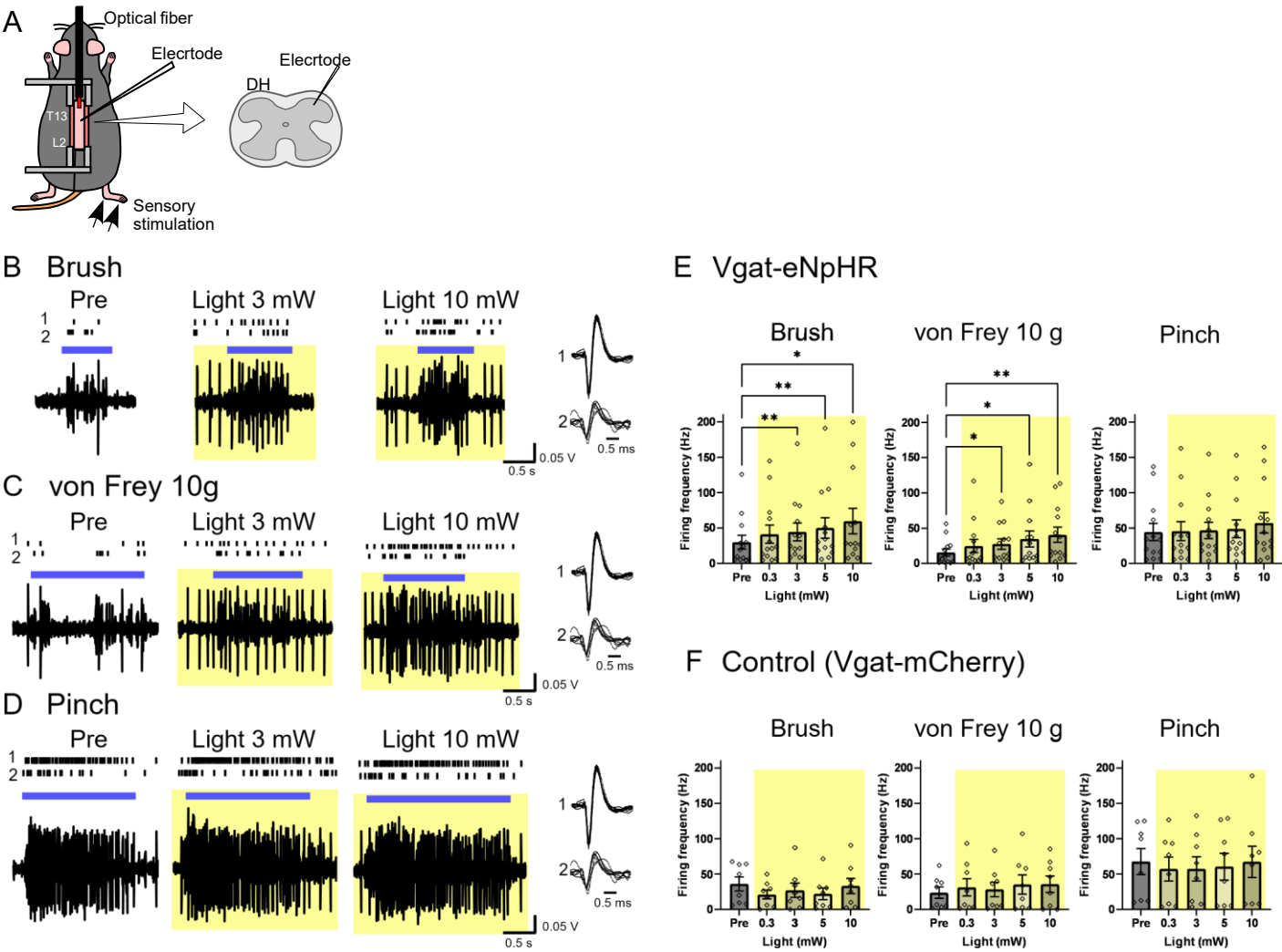


Figure4

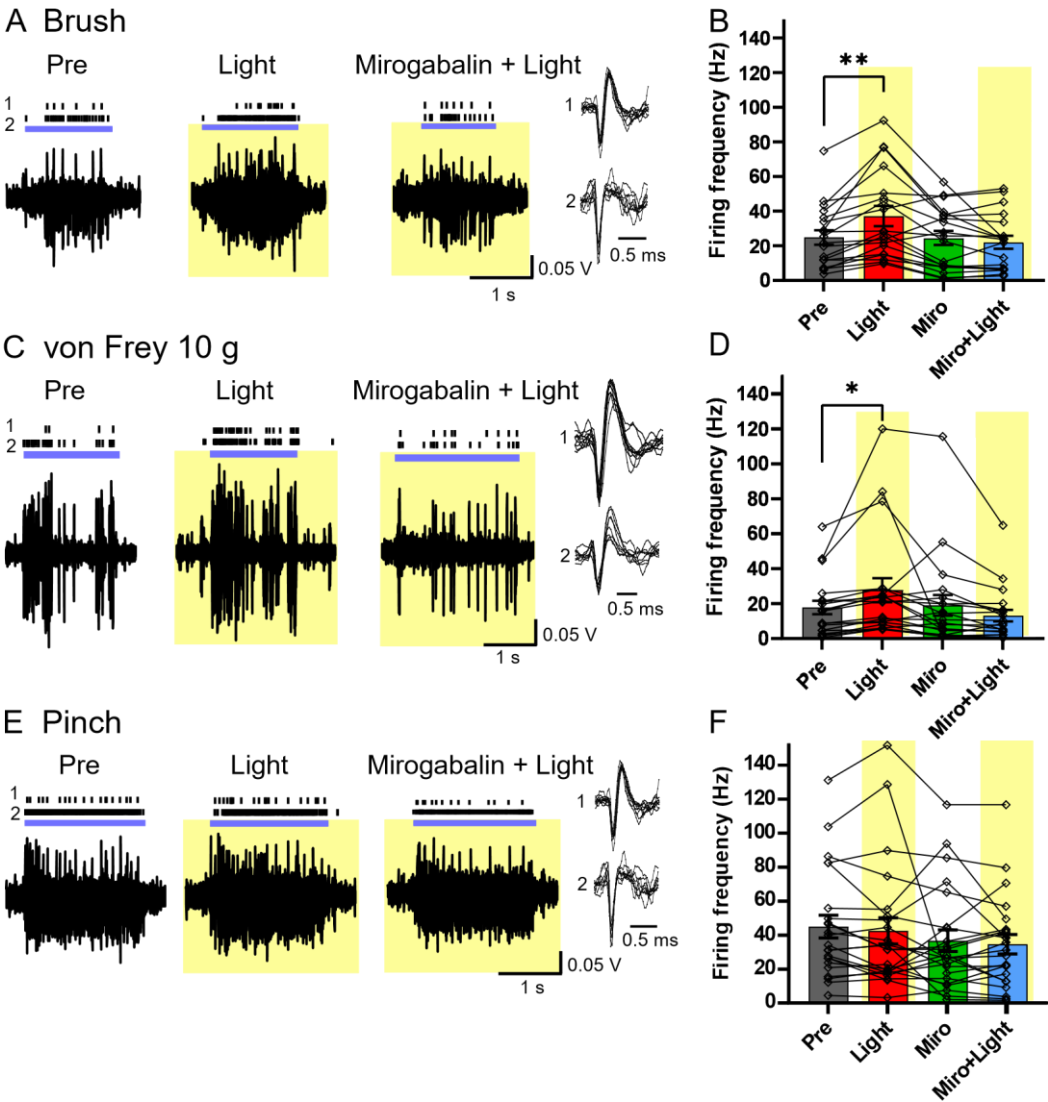


Figure5

